CrossMark

CARDIAC RADIOLOGY

Computed tomography of dynamic changes of the aortic root during systole and diastole in patients with coronary artery calcification

**Xiaohan Hu · Claudia Frellesen · Ralf W. Bauer ·
J. Matthias Kerl · Martin Beeres · Boris Bodelle ·
Thomas Lehnert · Thomas J. Vogl · Julian L. Wichmann**

Abstract

Purpose This study was done to investigate the dynamic changes of the aortic root during systole and diastole in patients with coronary artery calcification (CAC) using dual-source computed tomography (DSCT).

Materials and methods We retrospectively analysed 77 consecutive patients who underwent calcium-scoring and angiographic cardiac DSCT. The long- and short-axis dimensions, axis areas of the aortic annulus, sinotubular junction and ascending aorta at the level of the pulmonary trunk in diastole and systole were measured. Average dimensions and relative areal changes between diastole and systole (%RA) of aortic annulus, sinotubular junction and ascending aorta were compared.

Results Systolic and diastolic long- and short-axis dimensions of the aortic annulus in patients with CAC ($n = 44$) demonstrated statistically significant differences (27.00 ± 2.84 mm vs. 28.04 ± 2.62 mm; $P < 0.001$; 21.78 ± 2.55 mm vs. 20.88 ± 2.31 mm; $P < 0.001$), while differences in average diameters and areas of the aortic annulus were nonsignificant ($P > 0.586$). Systolic and diastolic axial areas of the sinotubular junction in patients with CAC demonstrated significant differences (7.21 ± 1.80 cm^2 vs. 6.92 ± 1.75 cm^2; $P < 0.001$). The %RA of the ascending aorta in patients with severe CAC (CAC score >400; $n = 15$) was significantly reduced compared to patients with minimal-to-moderate CAC (CAC score <400; $n = 29$; 4.77 ± 2.88 vs. 7.51 ± 3.81, $P = 0.014$).

Conclusions In comparison with patients without CAC, the long- and short-axis dimensions of the aortic annulus and areas of the sinotubular junction show significant differences during the cardiac cycle in patients with CAC. The presence of severe CAC significantly influences the flexibility of the wall of the ascending aorta.

Introduction

The aortic root is defined as an anatomical entity consisting of the aortic valve leaflets and attachments, the interleaflet trigones, the sinuses of Valsalva, the sinotubular junction, and the aortic annulus. Any changes in its structure may influence the structure of the heart and left ventricular function [1, 2]. Thus, evaluation of structural changes of the aortic root is crucial for preoperative assessment prior to cardiovascular surgery [3–5].

Prior studies have reported controversial results regarding the dynamic changes of the aortic root during the cardiac cycle. Most of the studies showed no dynamic changes in the human aortic root [6–8]. However, one study reported dynamic changes in the aortic root in healthy subjects detected by cardiac computed tomography (CT) [9]. Another study demonstrated differences in the dimensions of the aortic annulus in patients with severe aortic stenosis [10].

Coronary artery calcification (CAC) is a marker of coronary artery atherosclerotic burden and correlates with systemic vascular disease [11]. Therefore, calcium deposits of the coronary artery wall may have a direct influence on

X. Hu and C. Frellesen contributed equally to this work and share first authorship.

X. Hu · C. Frellesen · R. W. Bauer · J. M. Kerl · M. Beeres ·
B. Bodelle · T. Lehnert · T. J. Vogl · J. L. Wichmann (✉)
Department of Diagnostic and Interventional Radiology,
University Hospital Frankfurt, Theodor-Stern-Kai 7,
60590 Frankfurt am Main, Germany
e-mail: docwichmann@gmail.com

the aortic structure. To the best of our knowledge, so far no studies have evaluated the dynamic changes of the aortic root during the cardiac cycle in patients with CAC in comparison with patients without CAC. The potential of CT to detect changes of the aortic root in patients with CAC is unknown.

Thus, the purpose of this study was to investigate the dynamic changes of the aortic root during systole and diastole in patients with CAC using dual-source CT (DSCT) and to assess whether the presence of CAC has an impact on the aortic root.

Materials and methods

Study population

This retrospective study was approved by the institutional review board with a waiver for informed patient consent. Both the unenhanced coronary calcium scan and contrast-enhanced cardiac CT images obtained during dual-source coronary CT angiography (cCTA) from consecutive patients referred for cCTA at our institution were analysed. Patients with aortic stenosis, valvular heart disease, cardiomyopathy or atrial fibrillation, hypertension, and diabetes were excluded. Patients with a history of heart surgery, angioplasty, stent placement, or pulmonary ablation were also excluded from the study. The baseline demographic details of patients were retrieved from the hospital information system. Finally, 77 patients were included in this study. A history of CAD was determined based on prior cCTA or invasive coronary angiography demonstrating at least moderate coronary disease ($\geq$50 % stenosis in one or more coronary arteries.

Determination of CAC

All calcium scoring scans were performed using a second-generation 128-slice DSCT (Somatom Definition Flash, Siemens Healthcare, Forchheim, Germany). All scans ranged from the carina to the diaphragm, including the complete coronary tree. All scans were performed in the craniocaudal direction. A collimation of 128×0.6 mm was used, and pitch was set to 3.4. A prospective electrocardiogram (ECG)-gated dose-saving technique with a fixed tube voltage of 120 kV and a reference tube current output of 80 mAs were used. Automated tube current modulation and pulsing-window adaptation (CARE Dose 4D) were activated to reduce radiation exposure.

All calcium-scoring scan series were reviewed on a commercially available workstation (Syngo MMWP, Siemens Healthcare) using the dedicated calcium-scoring application. After each calcification was marked by an experienced

observer, the Agatston score was semi-automatically calculated using predefined parameters. For the purpose of this study, CAC was further divided into minimal-to-moderate (Agatston score of <400) and severe (>400) CAC.

Evaluation of the aortic root

After the calcium scoring scan, cCTA was performed using the same DSCT system. The tube voltage was fixed at 120 kV, and the tube current ranged from 100 to 300 mA using the same automated tube current modulation and pulsing-window adaptation algorithm. A collimation of 128×0.6 mm with a pitch of 0.34 was used. A nonionic contrast medium (Iomeprol; Imeron 400, Bracco Imaging, Konstanz, Germany) with a concentration of 400 mg/mL was administered at 5 mL/s through an antecubital vein of the right arm. The total amount of contrast volume was calculated depending on the patients' body weight (1 mL/kg). The scan delay time was determined using the test-bolus technique. ECG data were acquired for retrospective image reconstruction at the desired phase of the cardiac cycle at the same time. Based on the literature, 30–40 % and 70–75 % of the R–R interval represented the systolic and diastolic phase, respectively [6]. Using the best phase application, the best diastolic (65–77 %) and systolic (33–48 %) phases were reconstructed at a slice thickness of 0.75 mm and increment of 0.4 mm.

Aortic root structure measurements including the long- and short-axis dimensions, axial areas of the aortic annulus (Fig. 1), axial areas of the sinotubular junction (Fig. 2), and ascending aorta at the level of the pulmonary trunk (Fig. 3) in diastole and systole were performed. Each measurement was repeated three times by the same observer blinded to CACS, and the average was used for analysis. The average diameter of the aortic annulus was determined using the formula:

$$(\text{short} - \text{axis dimension} + \text{long} - \text{axis dimension})/2$$

The relative areal change (%RA) was calculated using the following formula:

$$\%RA = 100 \times (As - Ad)/Ad$$

where "As" refers to the biggest value of the area in diastole and systole, while "Ad" refers to the smallest value [12–14].

The best diastolic and systolic phase images were then analysed in the cine application on the same workstation. The endocardial and epicardial borders of the left ventricle were traced automatically on short- and long-axis images, but necessary manual adjustments were performed by the same observer if necessary. The stroke volume and ejection fraction were then automatically calculated.
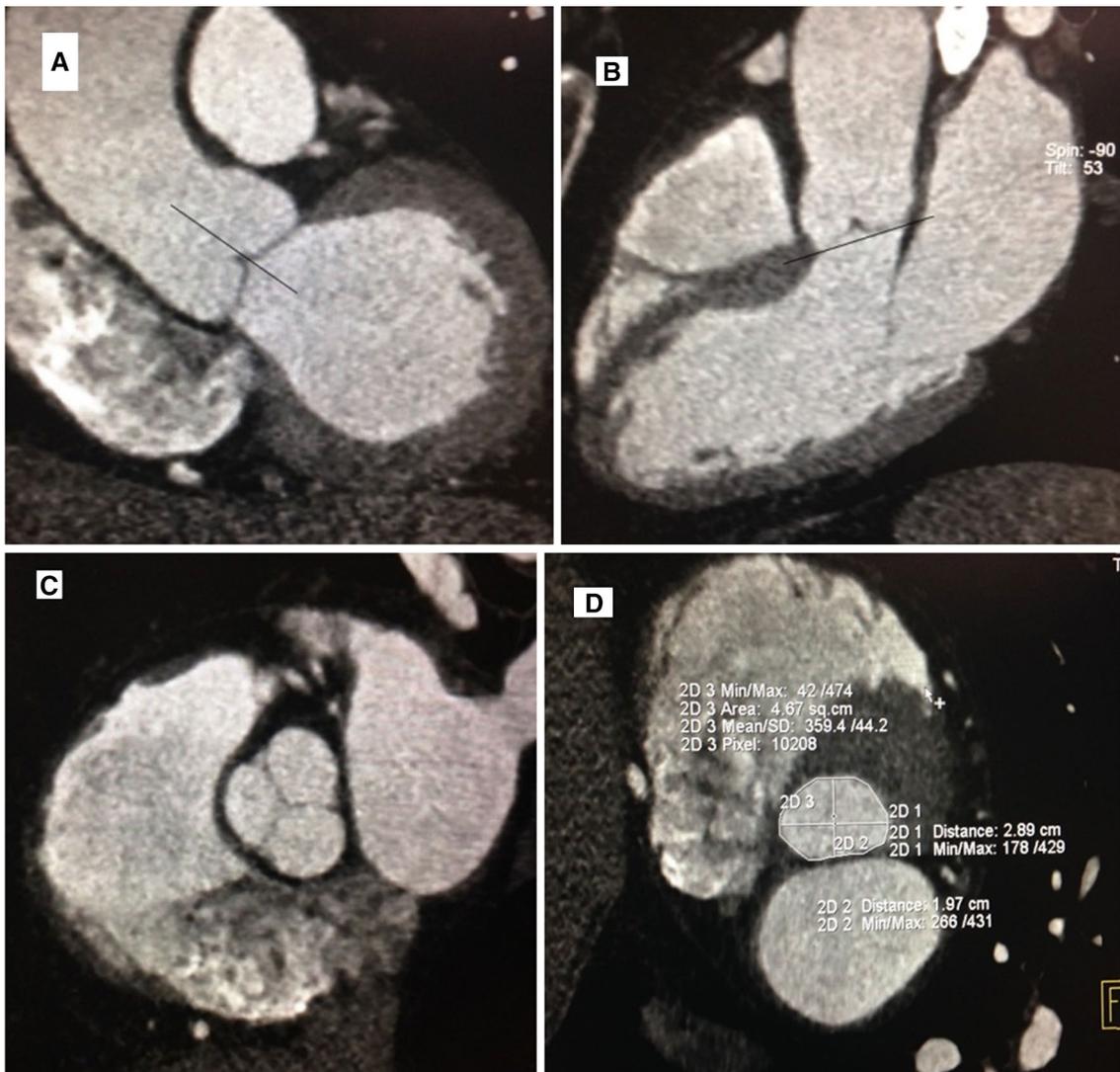
Fig. 1 Measurement of the aortic annulus. From the coronal projection (**a**), a vertically oriented oblique tool (*black line*) is placed to produce a sagittal oblique reconstruction. A transverse plane is then placed on the sagittal reconstruction (**b**) at the level of the commissures. This transverse plane yields a double oblique transverse image of the aortic annulus (**c**). The dataset is then scrolled through until the most caudal attachments of the aortic valve are identified (**d**).The nadirs of all three cusps have been identified on the transverse image, ensuring the appropriate plane for assessment of the aortic annulus. The long- and short-axis dimensions measure 28.9 mm and 19.7 mm, respectively, and the basal ring area measures 4.67 cm^2

Statistical analysis

All statistical analyses were performed using SPSS for Windows (version 17.0, SPSS, Chicago, IL, USA). Descriptive statistics are reported as mean $\pm$ standard deviation. The Chi square test was used to access the difference of categorical variables between the two groups. Statistical significances between the two groups were assessed by the independent sample t test. Statistical significances between diastole and systole were assessed using paired t tests. Values of $P < 0.05$ indicated a statistically significant difference.

Results

A total of 77 subjects (56 males and 21 females) with a mean age of 64 ± 12 years (range 40–88 years) were enrolled in this study. Image quality was considered diagnostic for all studies. Baseline characteristics including left ventricle function are shown in Table 1. From the sub-group analysis between patients with and without CAC (Table 1), no significant differences regarding age, gender, thoracic diameters, stroke volume, ejection fraction, or heart rate were observed between the two groups.
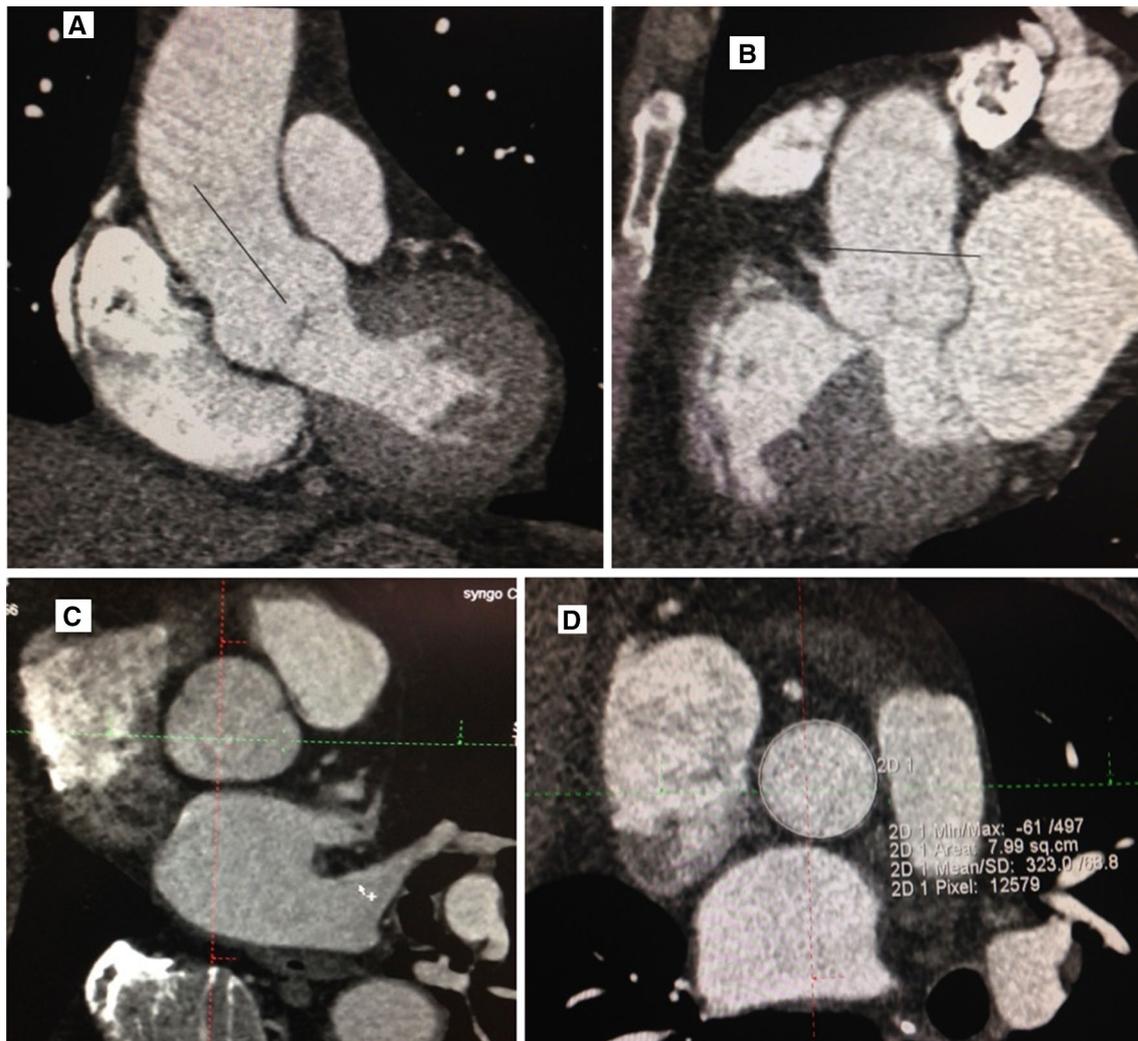
Fig. 2 Measurement of the sinotubular junction. From the coronal projection (**a**), a vertically oriented oblique plane is placed to produce a sagittal oblique reconstruction. A transverse plane is then placed in the sagittal reconstruction (**b**) at the level of the junction. The dataset is then scrolled through to yield a transverse image of all three sinuses (**c**), ensuring the appropriate plane for assessment of the sinotubular junction. The dataset is then scrolled until the most terminal attachments of the sinuses are identified (**d**). The direct measurement of the area is 7.99 cm^2

Comparison of the systolic and diastolic long- and short-axis dimensions of the aortic annulus in patients with CAC demonstrated significant differences compared to patients without CAC (27.00 ± 2.84 mm vs. 28.04 ± 2.62 mm, $P < 0.001$; 21.78 ± 2.55 mm vs. 20.88 ± 2.31 mm, $P < 0.001$), while there were no significant differences between the systolic and diastolic average diameter and area of the aortic annulus ($P = 0.605$ and $P = 0.586$, respectively).

Evaluation of the systolic and diastolic axial areas of the sinotubular junction in patients with CAC resulted in significant differences compared to patients without CAC (7.21 ± 1.80 cm^2 vs. 6.92 ± 1.75 cm^2; $P < 0.001$).

Comparisons of systolic and diastolic measurements of the aortic root in patients with CAC are summarised in Table 2. The mean diastolic long- and short-axis dimensions of the aortic annulus in patients with CAC were larger than in systole. The mean axial area of the sinotubular junction of patients with CAC in diastole was smaller than during systole. In patients without CAC, no dynamic changes were observed regarding the dimensions of the aortic annulus and areas of both aortic annulus and sinotubular junction (Table 2).

There were no significant differences in systolic and diastolic dimensions and areas of the aortic annulus and the sinotubular junction between patients with CAC and
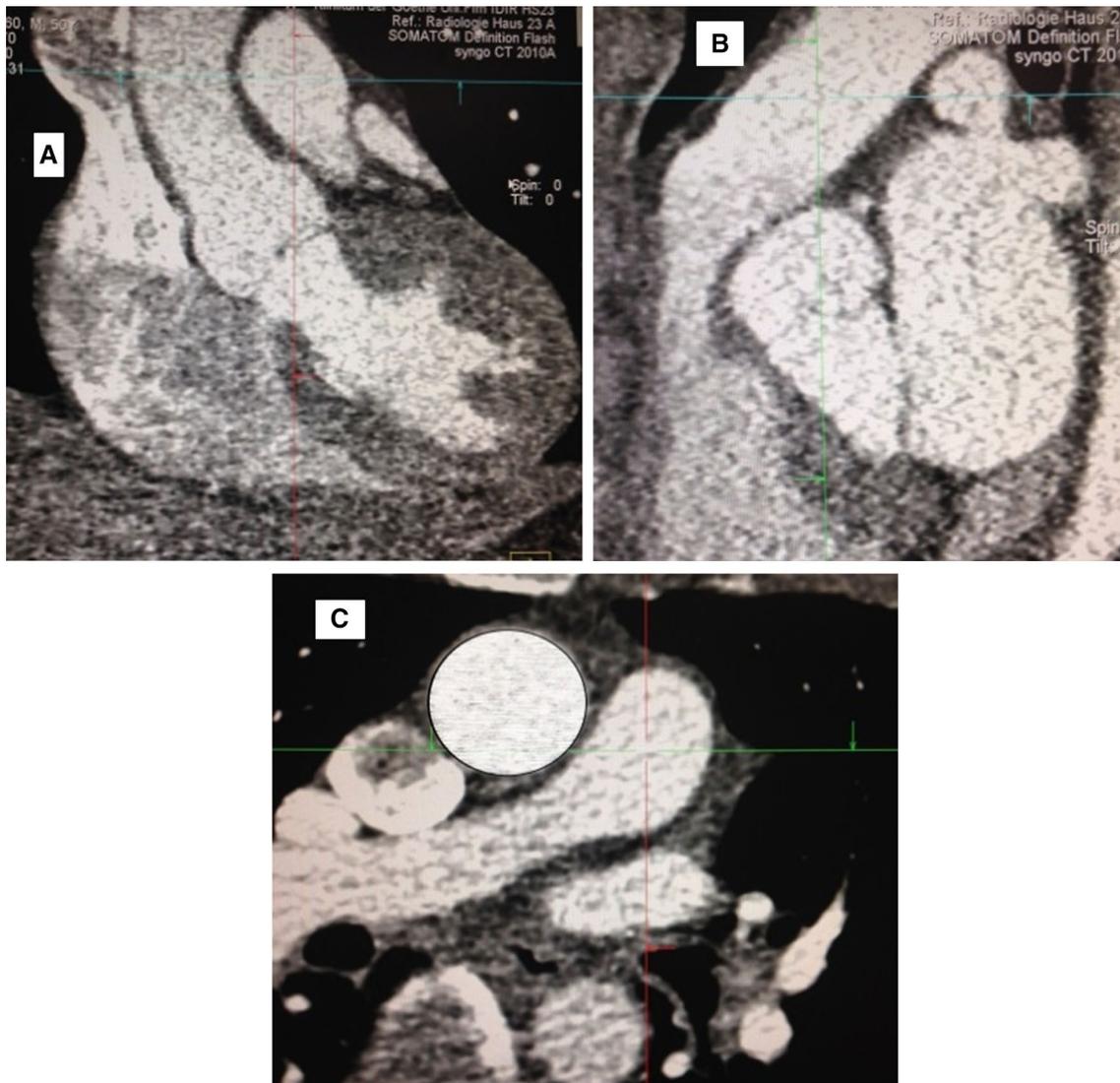
Fig. 3 Measurement of the ascending aorta at the level of the centre of the pulmonary trunk. Coronal (**a**), sagittal (**b**) and axial (**c**) views. The circumference is carefully traced, resulting in a direct measurement of the shaded area

Table 1 Patient characteristics

Variable	All patients ($n = 77$)	Patients		P
		Without CAC ($n = 33$)	With CAC ($n = 44$)	
Mean age $\pm$ SD (years)	64.2 ± 12.1	61.3 ± 13.3	65.2 ± 11.7	0.317
Female (n)	21 (27.27 %)	11 (33.33 %)	10 (22.73 %)	0.301
CAD (n)	32 (41.56 %)	2 (6.06 %)	30 (68.18 %)	<0.001
Thorax				
Left–right diameter (cm)	34.43 ± 3.47	33.96 ± 2.12	34.60 ± 3.85	0.535
Lateral diameter (cm)	28.54 ± 3.69	27.49 ± 2.63	28.91 ± 3.96	0.117
Stroke volume (mL)	66.65 ± 25.06	68.00 ± 19.82	66.26 ± 26.61	0.816
Ejection fraction (EF%)	53.22 ± 13.06	51.09 ± 12.16	53.84 ± 13.40	0.527
Heart rate (beats/min)	68 ± 11	72 ± 12	65 ± 11	0.092

Table 2 Comparison of systolic and diastolic measurements of the aortic root

Variable	Systolic	Diastolic	Difference		
			Mean	SD	P
With CAC ($n = 44$)					
Aortic annular					
Long-axis dimension (cm)	2.70 ± 0.28	2.80 ± 0.26	−0.10	0.10	<0.001
Short-axis dimension (cm)	2.18 ± 0.26	2.09 ± 0.23	0.09	0.15	<0.001
Average diameter (cm)	2.44 ± 0.25	2.45 ± 0.23	−0.01	0.69	0.605
Area (cm^2)	4.59 ± 0.90	4.55 ± 0.86	0.03	0.37	0.586
Sinotubular junction					
Area (cm^2)	7.21 ± 1.80	6.92 ± 1.75	0.29	0.32	<0.001
Without CAC ($n = 33$)					
Aortic annular					
Long-axis dimension (cm)	2.86 ± 0.31	2.93 ± 0.40	−0.07	0.24	0.237
Short-axis dimension (cm)	2.22 ± 0.25	2.12 ± 0.30	0.09	0.26	0.164
Average diameter (cm)	2.54 ± 0.23	2.53 ± 0.33	0.01	0.20	0.836
Area (cm^2)	5.02 ± 0.86	4.93 ± 1.15	0.09	0.59	0.543
Sinotubular junction					
Area (cm^2)	6.74 ± 1.60	6.63 ± 1.43	0.10	0.54	0.462

Table 3 Comparison of the aortic root in patients with and without CAC

Variable	Systolic			Diastolic		
	CAC	Without CAC	P	CAC	Without CAC	P
Aortic annular						
Long-axis dimension (mm)	27.00 ± 2.84	28.56 ± 3.11	0.090	28.04 ± 2.62	29.30 ± 3.99	0.254
Short-axis dimension (mm)	21.78 ± 2.55	22.16 ± 2.51	0.615	20.88 ± 2.31	21.21 ± 3.01	0.690
Average diameter(mm)	24.39 ± 2.52	25.36 ± 2.28	0.167	24.46 ± 2.29	25.26 ± 3.34	0.388
Area (cm^2)	4.59 ± 0.90	5.02 ± 0.86	0.097	4.55 ± 0.86	4.93 ± 1.15	0.252
Sinotubular junction						
Area (cm^2)	7.21 ± 1.80	6.74 ± 1.60	0.329	6.92 ± 1.75	6.63 ± 1.43	0.522

without CAC (Table 3). RA % of the ascending aorta at the level of the pulmonary trunk in patients with CAC did not significantly differ from patients without CAC (6.57 ± 3.72 % vs. 6.51 ± 4.54 %; $P = 0.950$).

The RA % of the ascending aorta at the level of the pulmonary trunk in patients with severe CAC was statistically smaller than in patients with minimal-to-moderate CAC (4.77 ± 2.88 % vs. 7.51 ± 3.81 %; $P = 0.014$). However, there were no statistically significant differences in RA % of the aortic annular and sinotubular junction. Comparisons of the patients with severe CAC and minimal-to-moderate CAC are shown in Table 4.

Discussion

The results of our study demonstrate that the long- and short-axis dimensions of the aortic annulus and area of the sinotubular junction in patients with CAC show significant changes during the cardiac cycle while no dynamic changes of the aortic root were observed in patients without CAC. The RA % of the ascending aorta at the level of the pulmonary trunk showed no significant differences between patients with and without CAC, but patients with severe CAC demonstrated a significantly smaller RA % of the ascending aorta compared to patients with minimal-to-moderate CAC.

Contrary findings have been reported regarding the dynamic changes of the aortic annulus and the sinotubular junction during the cardiac circle [9, 10]. This could be attributed to the different methods to measure these dimensions [15]. In addition, three-dimensional measurements have shown significant differences compared to two-dimensional measurements [9]. In our study, we evaluated the double oblique imaging plane for exact alignment with the aortic annulus as it has shown high inter- and intra-observer agreement [15]. In our study, no dynamic changes were observed regarding the aortic root in patients without CAC, which is in accordance with prior studies [6–8].

Table 4 Comparison of patients with minimal-to-moderate CAC and severe CAC

Variable	Patients		P
	With min-moderate CAC ($n = 29$)	With severe CAC ($n = 15$)	
Mean age $\pm$ SD (years)	63 $\pm$ 11	70 $\pm$ 11	0.066
Female (n)	8 (27.59 %)	2 (13.33 %)	0.490
CAD (n)	19 (65.52 %)	11 (73.33 %)	0.852
Thorax			
Left–right diameter (cm)	34.67 $\pm$ 3.48	34.46 $\pm$ 4.63	0.875
Lateral diameter (cm)	28.38 $\pm$ 4.02	29.95 $\pm$ 3.78	0.210
Stroke volume(mL)	66.22 $\pm$ 27.98	63.91 $\pm$ 25.52	0.808
EF%	52.70 $\pm$ 14.50	53.36 $\pm$ 12.44	0.889
Heart rate (beats/min)	68 $\pm$ 11	63 $\pm$ 9	0.123
Systole			
Aortic annular			
Long-axis dimension (mm)	26.95 $\pm$ 2.98	27.10 $\pm$ 2.62	0.860
Short-axis dimension (mm)	21.46 $\pm$ 2.76	22.41 $\pm$ 2.03	0.204
Average diameter (mm)	24.20 $\pm$ 2.73	24.75 $\pm$ 2.10	0.462
Area (cm^2)	4.51 $\pm$ 0.98	4.73 $\pm$ 0.72	0.390
Sinotubular junction			
Area (cm^2)	7.07 $\pm$ 1.80	7.49 $\pm$ 1.82	0.476
Diastole			
Aortic annular			
Long-axis dimension (mm)	28.25 $\pm$ 2.67	27.63 $\pm$ 2.55	0.459
Short-axis dimension (mm)	20.62 $\pm$ 2.57	21.37 $\pm$ 1.68	0.319
Average diameter (mm)	24.44 $\pm$ 2.46	24.50 $\pm$ 2.03	0.929
Area (cm^2)	4.54 $\pm$ 0.93	4.59 $\pm$ 0.73	0.835
Sinotubular junction			
Area (cm^2)	6.74 $\pm$ 1.69	7.26 $\pm$ 1.87	0.375
%RA			
Aortic annular	7.08 $\pm$ 5.74	8.02 $\pm$ 5.74	0.609
Sinotubular junction	5.18 $\pm$ 3.76	4.60 $\pm$ 5.03	0.698
Ascending aorta	7.51 $\pm$ 3.81	4.77 $\pm$ 2.88	0.014

In patients with CAC the long- and short-axis dimensions of the aortic annulus showed significant changes during the cardiac cycle. In addition, systolic and diastolic axial areas of the sinotubular junction demonstrated significant differences. These changes likely result in decreased flexibility of the aorta [16]. In the present study, this was indicated by a significantly reduced RA % of the aorta at the level of the pulmonary trunk in patients with severe CAC compared to patients with minimal-to-moderate CAC ($P = 0.014$). We assessed the RA % as an indicator of vessel elasticity [13], since elasticity is influenced by manifestation of adverse functional changes within the vessel wall [17]. Prior studies suggested that the reduction of arterial elasticity is a sign of vessel dysfunction [18]. CAC was reported to be strongly correlated with systemic vascular dysfunction [19], indicating its association with aortic elasticity. However, we did not observe significant differences regarding RA % of the sinotubular junction between patients with severe and minimal-to-moderate CAC. This may be explained by the fact that less elastic tissue is present in that segment of the vascular wall [8].

A previous study reported that the mean diameter of the sinotubular junction enlarges with increasing age, but the aortic annulus diameter shows better correlation with body surface area compared to age, especially in a younger population [20]. In our study, there was no significant difference regarding age and gender between both groups. We evaluated stroke volume, ejection fraction, and heart rate to assess cardiac function and patient characteristics. Several prior studies have shown that left ventricular function assessed by cardiac CT shows good reproducibility and correlation compared to two-dimensional transthoracic echocardiography and magnetic resonance imaging [21–23].

This study had some limitations, mainly due to its retrospective study design evaluating a relatively small number of

of patients. Moreover, lipid or glucose serum levels, current or prior tobacco and alcohol consumption, and drug use were not evaluated as such data could not be obtained from the electronic medical chart system for all patients. Furthermore, since detailed data regarding body weight and height were also not available for most patients, thoracic diameters were measured in an attempt to compensate this limitation. In addition, aortic and aortic root calcification was not evaluated.

In conclusion, long- and short-axis dimensions of the aortic annulus and area of the sinotubular junction show significant changes during systole and diastole in patients with CAC. The presence of severe CAC results in a restriction of the flexibility of the wall of the ascending aorta measured by a reduced %RA, indicating a complex vascular pathophysiological cascade in patients with extensive CAC. Although additional studies are necessary to evaluate the long-term clinical outcome of these findings, these initial results indicate that severe CAC may also be a potential indicator of extracardiac vascular disease, potentially further influencing patient outcome [2].

References

1. Lam CS, Gona P, Larson MG et al (2013) Aortic root remodeling and risk of heart failure in the Framingham Heart study. JACC Heart Fail 1(1):79–83
2. Gardin JM, Arnold AM, Polak J (2006) Usefulness of aortic root dimension in persons > or = 65 years of age in predicting heart failure, stroke, cardiovascular mortality, all-cause mortality and acute myocardial infarction (from the Cardiovascular Health Study). Am J Cardiol 97(2):270–275
3. Marom G, Haj-Ali R, Rosenfeld M et al (2013) Aortic root numeric model: annulus diameter prediction of effective height and coaptation in post-aortic valve repair. J Thorac Cardiovasc Surg 145(2):406–411.e1
4. Zhu D, Zhao Q (2011) Dynamic normal aortic root diameters: implications for aortic root reconstruction. Ann Thorac Surg 91(2):485–489
5. Losenno KL, Gelinas JJ, Johnson M, Chu MWA (2013) Defining the efficacy of aortic root enlargement procedures: a comparative analysis of surgical techniques. Can J Cardiol 29(4):434–440
6. Tops LF, Wood DA, Delgado V et al (2008) Noninvasive evaluation of the aortic root with multislice computed tomography implications for transcatheter aortic valve replacement. JACC Cardiovasc Imaging 1(3):321–330
7. Wood DA, Tops LF, Mayo JR et al (2009) Role of multislice computed tomography in transcatheter aortic valve replacement. Am J Cardiol 103(9):1295–1301
8. Kazui T, Izumoto H, Yoshioka K, Kawazoe K (2006) Dynamic morphologic changes in the normal aortic annulus during systole and diastole. J Heart Valve Dis 15(5):617–621
9. De Heer LM, Budde RPJ, Mali WPTM et al (2011) Aortic root dimension changes during systole and diastole: evaluation with ECG-gated multidetector row computed tomography. Int J Cardiovasc Imaging 27(8):1195–1204
10. Bertaso AG, Wong DT, Liew GY et al (2012) Aortic annulus dimension assessment by computed tomography for transcatheter aortic valve implantation: differences between systole and diastole. Int J Cardiovasc Imaging 28(8):2091–2098
11. O'Rourke RA, Brundage BH, Froelicher VF et al (2000) American College of Cardiology/American Heart Association Expert Consensus Document on electron-beam computed tomography for the diagnosis and prognosis of coronary artery disease. J Am Coll Cardiol 36(1):326–340
12. Vriz O, Driussi C, Bettio M et al (2013) Aortic root dimensions and stiffness in healthy subjects. Am J Cardiol 112(8):1224–1229
13. Li N, Beck T, Chen J et al (2011) Assessment of thoracic aortic elasticity: a preliminary study using electrocardiographically gated dual-source CT. Eur Radiol 21(7):1564–1572
14. Gurvitch R, Webb JG, Yuan R et al (2011) Aortic annulus diameter determination by multidetector computed tomography: reproducibility, applicability, and implications for transcatheter aortic valve implantation. JACC Cardiovasc Interv 4(11):1235–1245
15. Schuhbaeck A, Achenbach S, Pflederer T et al (2014) Reproducibility of aortic annulus measurements by computed tomography. Eur Radiol 24(8):1878–1888
16. Nelson AJ, Worthley SG, Cameron JD et al (2009) Cardiovascular magnetic resonance-derived aortic distensibility: validation and observed regional differences in the elderly. J Hypertens 27(3):535–542
17. Cavalcante JL, Lima JAC, Redheuil A, Al-Mallah MH (2011) Aortic stiffness: current understanding and future directions. J Am Coll Cardiol 57(14):1511–1522
18. Ahmadi N, Nabavi V, Hajsadeghi F et al (2011) Impaired aortic distensibility measured by computed tomography is associated with the severity of coronary artery disease. Int J Cardiovasc Imaging 27(3):459–469
19. Ahmadi N, Hajsadeghi F, Gul K et al (2008) Relations between digital thermal monitoring of vascular function, the Framingham risk score, and coronary artery calcium score. J Cardiovasc Comput Tomogr 2(6):382–388
20. Son MK, Chang SA, Kwak JH et al (2013) Comparative measurement of aortic root by transthoracic echocardiography in normal Korean population based on two different guidelines. Cardiovasc Ultrasound 11:28
21. Sieslack AK, Dziallas P, Nolte I, Wefstaedt P (2013) Comparative assessment of left ventricular function variables determined via cardiac computed tomography and cardiac magnetic resonance imaging in dogs. Am J Vet Res 74(7):990–998
22. Raman SV, Shah M, McCarthy B et al (2006) Multi-detector row cardiac computed tomography accurately quantifies right and left ventricular size and function compared with cardiac magnetic resonance. Am Heart J 151(3):736–744
23. Takx RA, Moscariello A, Schoepf UJ et al (2012) Quantification of left and right ventricular function and myocardial mass: comparison of low-radiation dose 2nd generation dual-source CT and cardiac MRI. Eur J Radiol 81(4):e598–e604